

RESEARCH ARTICLE

Open Access



Comparative analysis of plant immune receptor architectures uncovers host proteins likely targeted by pathogens

Panagiotis F. Sarris^{1,3†}, Volkan Cevik^{1†}, Gulay Dagdas¹, Jonathan D. G. Jones¹ and Ksenia V. Krasileva^{1,2*}

Abstract

Background: Plants deploy immune receptors to detect pathogen-derived molecules and initiate defense responses. Intracellular plant immune receptors called nucleotide-binding leucine-rich repeat (NLR) proteins contain a central nucleotide-binding (NB) domain followed by a series of leucine-rich repeats (LRRs), and are key initiators of plant defense responses. However, recent studies demonstrated that NLRs with non-canonical domain architectures play an important role in plant immunity. These composite immune receptors are thought to arise from fusions between NLRs and additional domains that serve as “baits” for the pathogen-derived effector proteins, thus enabling pathogen recognition. Several names have been proposed to describe these proteins, including “integrated decoys” and “integrated sensors”. We adopt and argue for “integrated domains” or NLR-IDs, which describes the product of the fusion without assigning a universal mode of action.

Results: We have scanned available plant genome sequences for the full spectrum of NLR-IDs to evaluate the diversity of integrations of potential sensor/decoy domains across flowering plants, including 19 crop species. We manually curated wheat and brassicas and experimentally validated a subset of NLR-IDs in wild and cultivated wheat varieties. We have examined NLR fusions that occur in multiple plant families and identified that some domains show re-occurring integration across lineages. Domains fused to NLRs overlap with previously identified pathogen targets confirming that they act as baits for the pathogen. While some of the integrated domains have been previously implicated in disease resistance, others provide new targets for engineering durable resistance to plant pathogens.

Conclusions: We have built a robust reproducible pipeline for detecting variable domain architectures in plant immune receptors across species. We hypothesize that NLR-IDs that we revealed provide clues to the host proteins targeted by pathogens, and that this information can be deployed to discover new sources of disease resistance.

Keywords: Genomics, Plant innate immunity, NLRs, Integrated domains, Gene fusions

Background

Plants recognize pathogens through an innate immune system that monitors pathogen-associated molecules either outside or inside the plant cell [1–4]. Pathogen-derived molecules known to trigger immunity are commonly classified into pathogen-associated molecular patterns (PAMPs), such as bacterial flagellin or fungal chitin, which are usually presented in the apoplast

space, and pathogen-derived effectors, which are more diverse and often translocated inside the host. Effectors are commonly deployed by the pathogen to target intracellular host proteins for effective nutrient delivery or suppression of plant defense responses. The two major branches of plant immunity, PAMP-triggered immunity (PTI) and effector-triggered immunity (ETI), are defined based on the type and location of the receptor, the molecule(s) detected, and downstream signaling components. PTI commonly employs receptor-like kinases or receptor-like proteins that detect PAMPs outside of plant cells and transmit signals within the cell via phosphorylation cascades that involve mitogen-activated protein kinase signaling cascades and other protein kinases

* Correspondence: Ksenia.Krasileva@tgac.ac.uk

†Equal contributors

¹The Sainsbury Laboratory, Norwich Research Park, Norwich, UK

²The Genome Analysis Centre, Norwich Research Park, Norwich, UK

Full list of author information is available at the end of the article

[5, 6]. ETI is initiated by plant receptors called nucleotide-binding leucine-rich repeat (NLR) proteins, which detect the presence of pathogen-derived effectors within plant cells and activate defense via as yet poorly understood mechanisms [2, 4]. Since one of the functions of the effectors inside plant cells is to disarm plant defense responses, there is a constant evolutionary arms race between pathogen effectors and components of plant immunity. This puts immense selection on pathogen effector genes [7–9] and on the effector targets and immune receptors in the plant [10–12]. Plant receptors evolve rapidly via various mechanisms, including point mutations, gene duplications and gene rearrangements [13, 14].

NLR-encoding genes are found from flowering plants to mosses [15–17]. All NLRs share a central nucleotide-binding (NB) domain, corresponding to the NB-ARC domain in Pfam. The NB domain is usually, but not always, associated with carboxy-terminal leucine-rich repeats (LRRs) and amino-terminal coiled coil (CC) or Toll/interleukin-1 receptor/resistance protein (TIR) domains [13, 18]. Although NLRs derive their name from having both NB and LRR domains, there have been several reports of disease resistance genes encoding proteins that lack LRRs [16, 19, 20]. Moreover, analyses of *Arabidopsis thaliana* RRS1 and rice (*Oryza sativa*) RGA4/Pik-1 have revealed the functional significance of additional domains present in some NLR proteins [21–25]. Therefore, plant NLRs support flexible architectures, perhaps to enable recognition of a broader range of pathogen-derived molecules.

Effectors can be recognized either through direct interaction with the NLR receptor (direct recognition) or through monitoring of an effector's activity on host proteins (indirect recognition) [4]. Although originally sparse, reports of the direct interaction between NLR and effector proteins have been growing in recent years, and include NLR proteins encoded by the rice *Pi-ta*, *RGA5* and *PiK* genes [24–26, 27], the *Nicotiana tabacum* *N* gene [28], the flax (*Linum usitatissimum*) *L5/L6* and *M* genes [29, 30], the *Arabidopsis* *RPP1* gene [31], and potato (*Solanum tuberosum*) *Rpi-blb1* [32]. Indirect recognition has been well-demonstrated for many immune receptors [33–36]. In this case, the receptor protein monitors host proteins, known as “guardees” if they actively contribute to immunity or “decoys” if they mimic the authentic host target. Binding and/or modification of such a guardee/decoy by an effector leads to activation of the NLR receptor [37]. For example, the status of RIN4 protein (RPM1 interacting protein 4) is monitored by at least two independent *Arabidopsis* NLRs, RPS2 and RPM1, which detect cleavage or phosphorylation of RIN4 by bacterial effectors AvrRpt2 and AvrRpm1 (or AvrB), respectively [34, 38, 39]. Similarly, an *Arabidopsis* NLR

protein RPS5 detects cleavage of a protein kinase PBS1 by bacterial cysteine protease effector AvrPphB [40]. A tomato (*Solanum lycopersicum*) protein kinase Pto interacts with effector AvrPto and is guarded by NLR protein Prf [41, 42].

Recent findings show that an NLR and a host protein involved in indirect recognition can be fused together. Specifically, NLR receptors can carry an additional protein domain, enabling perception of pathogen effectors. Such recognition mode is known as “the integrated decoy/sensor” model [43, 44] and is based on three examples of NLRs with integrated domains (NLR-IDs) and mechanistic insights into their activity: *Arabidopsis* NLR protein RRS1 carries an additional WRKY domain [21, 22]; and rice RGA5 and Pik-1 proteins are fused to heavy metal-associated (HMA, also known as RATX1) domains [23–25]. The acetyltransferase effector PopP2, from the wilt pathogen *Ralstonia solanacearum*, and the effector AvrRps4, from the leaf pathogen *Pseudomonas syringae* pv. *pisi*, are both recognized upon their interaction with or modification of the WRKY DNA-binding domain of RRS1 protein. Furthermore, both effectors target several WRKY transcription factors in *Arabidopsis*, which indicates that the RRS1-WRKY domain has evolved as a trap for the perception of effectors that target WRKY transcription factors. Similarly to RPS4/RRS1, the rice CC-NB-LRR receptor pair RGA4/RGA5 recognizes two unrelated effectors, AVR-Pia and AVR1-CO39 of *Magnaporthe oryzae*, upon their direct interaction with the C-terminus of RGA5 [27]. Interestingly, the recognition of both effectors by RGA5 occurs through a small C-terminal HMA domain, also related to the cytoplasmic copper chaperone RATX1 from *Saccharomyces cerevisiae* [27]. As for RGA4/RGA5, the CC-NB-LRR receptor pair Pik-1/Pik-2, which contains the HMA domain fused between the CC and the NB-ARC regions of Pik-1, binds Avr-Pik effector of *M. oryzae* to activate immunity [23–25]. However, to date there are no published reports of other HMA domain proteins being targeted by AVR-Pia, AVR1-CO39 and AVR-Pik, although rice Pi21 is a HMA protein that confers susceptibility to the rice blast fungus [45].

The availability of sequenced plant genomes allowed us to test if integration of new domains in NLRs is widespread in angiosperms. We have examined NLR domain architectures from 40 publicly available plant predicted proteomes, and identified 720 NLR-IDs that involved both recently formed and conserved or recurrent fusions. A previous screen performed by Cesari et al. revealed a total of 22 unique integrated-domain fusions to NLR proteins [43]. This was based on a BLAST search carried out using two previously identified NLR proteins, RGA5 and RRS1, as “baits”. This work formed an important preliminary basis for the current study. Here, we have built a high-

throughput reproducible pipeline that can be applied to any newly sequenced set of predicted proteins for genome-wide identification of NLR-IDs. We have applied our pipeline in combination with the manual verification to 40 plant genomes, including mosses and flowering plants (monocots and dicots), to discover 265 unique NLR integrated-domains, including the ones that have been already described by Cesari et al. [43]. This is necessarily an underestimate since protein annotations of public datasets are often incomplete [46]; therefore, our easily adopted reproducible methodology is key to expanding these analyses even further once more data becomes available. We examined which NLR-IDs occurred in multiple plant families suggesting their conservation and functional significance. Availability of published effector interactome screens [47, 48] allowed us to overlay our analyses with predicted effector targets. Our analysis revealed that extraneous domains have repeatedly integrated into NLR proteins across all plant lineages. Some of the integrated domains are already known to be implicated in pathogen defense; for example, RIN4, NPR1. Other integrated domains originated from host proteins that may function in pathogen interactions, and are prime candidates for functional analysis to engineer disease-resistant plants.

Results and discussion

Identification of NLR proteins in plants based on the conserved NB-ARC domain

To gain insight into the evolution and diversity of NLR protein architectures across plants, we performed annotation of the Pfam NB-ARC domain-containing proteins in predicted proteomes of 40 publicly available plant species, which include algae, mosses as well as diverse families across angiosperms. (Fig. 1, Additional file 1). We have assembled a pipeline to annotate the domains present in the predicted proteomes of each species, and extracted NB-ARC-containing proteins as well as any other domain associated with it (Additional files 2 and 3). The current Pfam NB-ARC domain model (PF00931) works well for detecting NLR genes in monocots as well as dicots as it includes 151 monocot and 242 dicot species used to build the hidden Markov model. Benchmarking on *Arabidopsis* showed that the NB-ARC domain is specific to NLR proteins with 169 proteins detected (215 splice variants), including 149 previously published NLR sequences [13] and 20 NB-ARC-containing proteins with no LRRs, and no false positive other ATPases detected. This showed the NB-ARC domain alone is a good predictor of NLRs. The performance of Pfam NB-ARC on monocot genomes has been validated previously, i.e. Steuernagel et al. looked at sensitivity of HMMER NB-ARC searches in *Brachypodium* [49]. We filtered for the top Pfam hit for each non-

overlapping protein region to ensure that only genes for which the NB-ARC domain scored higher than other ATPase-related domains were retained. As annotations of many plant species are currently fragmented, we did not require LRR presence to be a strict criterion and included all NB-containing proteins for further analyses. Altogether, we have identified 14,363 NB-ARC-containing proteins across all species (Fig. 1, Additional files 4 and 5). Of these, 720 proteins had additional domains not typical for NLR proteins (Fig. 1, Additional files 3, 6 and 7).

We have manually analyzed NLR-IDs in *Brassica napus*, *Brassica rapa*, *S. lycopersicum*, *Medicago truncatula*, *Brachypodium distachyon* and *Triticum urartu* by cross-checking the sequences against UniProtKB and Swiss-Prot databases, and were able to validate the accuracy of >95 % of high-throughput predictions (Additional file 8). Our manual analyses of NLR-IDs in wild wheatgrass (*T. urartu*) showed that there were only 3 out of 44 proteins that we predicted as NLRs and do not appear to carry a canonical NB-ARC domain showing a very low rate of false positive predictions even in genomes of monocots.

Similar to previous reports, our data show that the NB-ARC domain appears as early as mosses and is present across all surveyed angiosperms (Fig. 1). In many lineages, the increase in NB-ARC domain-containing proteins is associated with polyploidy or ancient polyploidization events (Fig. 1) [50, 51]; i.e. 1,224 NB-ARC genes in hexaploid wheat (*Triticum aestivum*), and 1,032 and 1,074 NB-ARC genes in recently duplicated apple (*Malus domestica*) and *M. truncatula* genomes, respectively [52–54]. The increase in R-genes in grasses is also likely linked to three ancient polyploidization events in its evolutionary history [50, 51]. A notable exception is maize (*Zea mays*), which contains only 191 NB-ARC proteins despite recent whole genome duplications. An unusually low number of NB-ARC-containing genes was detected in papaya (*Carica papaya*, 56 NB-ARC genes) and cucumber (*Cucumis sativus*, 76 NB-ARC genes) for which there is no clear explanation.

Distinct class of TIR domain is present in all flowering plants

Our bioinformatics pipeline discovers any combinations of protein family domains within Pfam present together with NB-ARC. The canonical TIR-NB domain combination is present widely in association with NB-ARC in mosses as well as dicots (Fig. 1). In monocots, our analyses confirmed the absence of canonical TIR, but we discovered that a distinct related domain (Pfam domain TIR_2) is present in both monocots and dicots, and the number of family members in each species is restricted to 2–5 genes (Fig. 1). These monocot and dicot TIR2

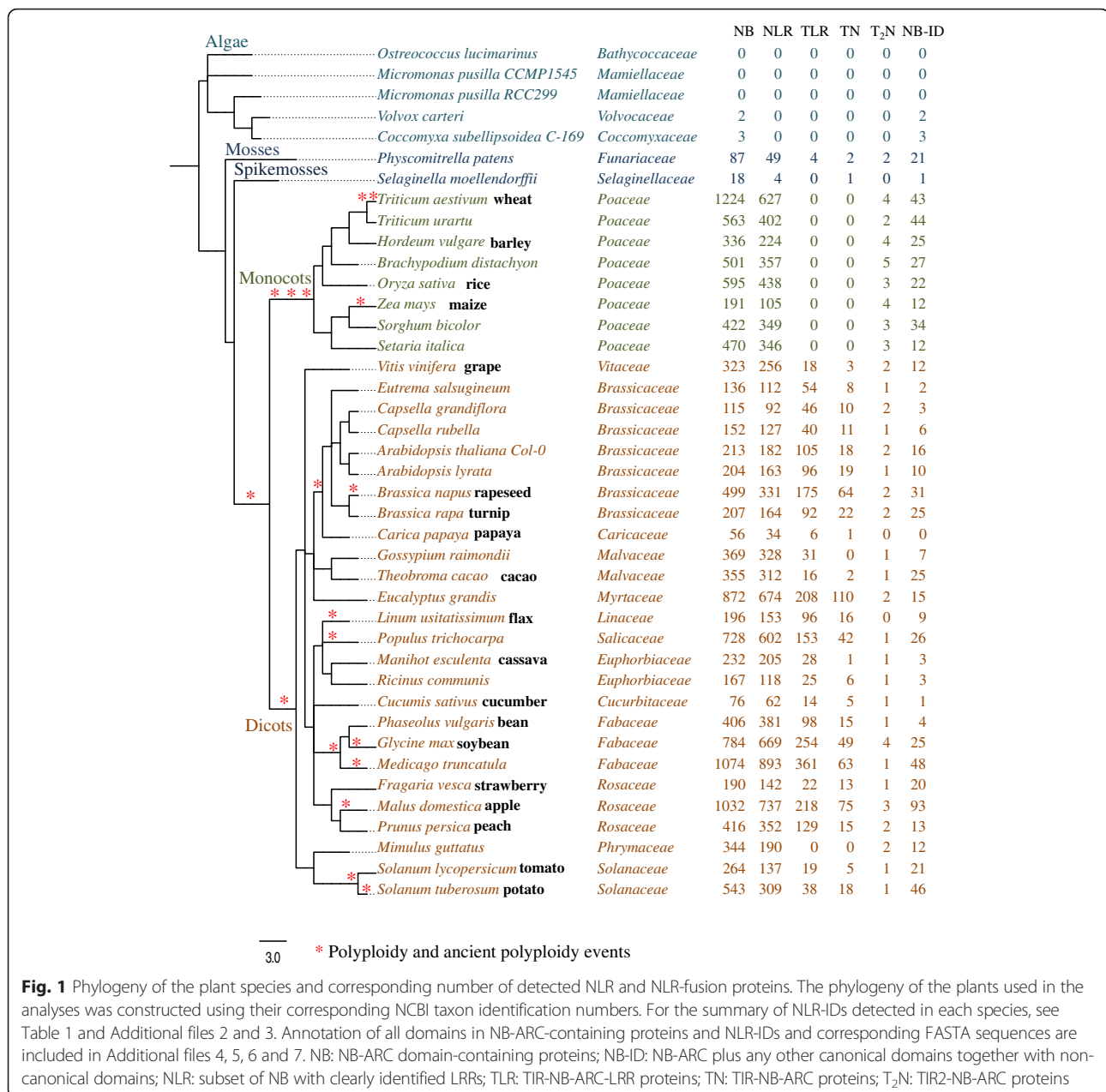


Fig. 1 Phylogeny of the plant species and corresponding number of detected NLR and NLR-fusion proteins. The phylogeny of the plants used in the analyses was constructed using their corresponding NCBI taxon identification numbers. For the summary of NLR-IDs detected in each species, see Table 1 and Additional files 2 and 3. Annotation of all domains in NB-ARC-containing proteins and NLR-IDs and corresponding FASTA sequences are included in Additional files 4, 5, 6 and 7. NB: NB-ARC domain-containing proteins; NB-ID: NB-ARC plus any other canonical domains together with non-canonical domains; NLR: subset of NB with clearly identified LRRs; TLR: TIR-NB-ARC-LRR proteins; TN: TIR-NB-ARC proteins; T₂N: TIR2-NB-ARC proteins

sequences form an ancient gene family that is evolutionarily distinct from the classic TIR sequences in dicots, consistent with previous analyses suggested by Nandety et al. [20]. We propose that this family shall be recognized separately as TIR2 NLRs and not grouped with canonical TIR proteins.

It is noteworthy that TIR2 domain proteins are also present in bacteria [55] and have been studied as important virulence factors in mammalian bacterial pathogens. TIR2 domain proteins from several mammalian pathogenic species suppress animal TLR-dependent host defenses by targeting TIR2-type mammalian innate immunity proteins [56]. We have looked for and identified

TIR2 domain proteins in many plant pathogenic bacteria (Additional file 9). Till now, there is no evidence regarding the role of these proteins in pathogenicity, yet the presence of TIR2 proteins both in plants and in phytopathogenic bacteria could indicate their involvement in pathogenicity similar to mammalian systems.

Fusion of NLRs to new domains is widespread across flowering plants

We found evidence of NLR-ID fusions in mosses and across all lineages of flowering plants. The number of NLR-IDs ranged from just 1 gene in cucumber (*C. sativus*) to 93 in apple (*M. domestica*) (Fig. 1, Table 1,

Table 1 Most prevalent integrated domains in flowering plants

| Integrated domain ^a | Species | Families | Domain description |
|--------------------------------|--|---|---|
| Pkinase | <i>A. thaliana</i> , <i>B. distachyon</i> , <i>B. napus</i> , <i>B. rapa</i> , <i>F. vesca</i> , <i>H. vulgare</i> , <i>M. domestica</i> , <i>M. guttatus</i> , <i>M. truncatula</i> , <i>O. sativa</i> , <i>P. patens</i> , <i>S. bicolor</i> , <i>S. italica</i> , <i>T. cacao</i> , <i>T. aestivum</i> , <i>T. urartu</i> , <i>V. vinifera</i> , <i>Z. mays</i> | <i>Brassicaceae</i> , <i>Fabaceae</i> , <i>Funariaceae</i> , <i>Malvaceae</i> , <i>Phrymaceae</i> , <i>Poaceae</i> , <i>Rosaceae</i> , <i>Vitaceae</i> | Protein kinase domain |
| DUF3542 | <i>L. usitatissimum</i> , <i>M. domestica</i> , <i>M. esculenta</i> , <i>M. guttatus</i> , <i>O. sativa</i> , <i>P. persica</i> , <i>P. trichocarpa</i> , <i>S. italica</i> , <i>S. lycopersicum</i> , <i>S. tuberosum</i> , <i>V. vinifera</i> | <i>Euphorbiaceae</i> , <i>Linaceae</i> , <i>Phrymaceae</i> , <i>Poaceae</i> , <i>Rosaceae</i> , <i>Salicaceae</i> , <i>Solanaceae</i> , <i>Vitaceae</i> | Protein of unknown function (DUF3542) |
| Pkinase_Tyr | <i>B. distachyon</i> , <i>B. napus</i> , <i>B. rapa</i> , <i>F. vesca</i> , <i>G. max</i> , <i>H. vulgare</i> , <i>M. domestica</i> , <i>O. sativa</i> , <i>P. patens</i> , <i>S. bicolor</i> , <i>T. cacao</i> , <i>T. aestivum</i> , <i>T. urartu</i> , <i>V. vinifera</i> | <i>Brassicaceae</i> , <i>Fabaceae</i> , <i>Funariaceae</i> , <i>Malvaceae</i> , <i>Poaceae</i> , <i>Rosaceae</i> , <i>Vitaceae</i> | Protein tyrosine kinase |
| WRKY | <i>A. lyrata</i> , <i>A. thaliana</i> , <i>B. distachyon</i> , <i>C. grandiflora</i> , <i>C. rubella</i> , <i>G. max</i> , <i>H. vulgare</i> , <i>M. domestica</i> , <i>S. bicolor</i> , <i>S. italica</i> , <i>T. cacao</i> , <i>T. aestivum</i> , <i>T. urartu</i> | <i>Brassicaceae</i> , <i>Fabaceae</i> , <i>Malvaceae</i> , <i>Poaceae</i> , <i>Rosaceae</i> | WRKY DNA-binding domain |
| RVT_3 | <i>F. vesca</i> , <i>G. max</i> , <i>M. domestica</i> , <i>M. esculenta</i> , <i>P. vulgaris</i> , <i>T. cacao</i> , <i>T. urartu</i> | <i>Euphorbiaceae</i> , <i>Fabaceae</i> , <i>Malvaceae</i> , <i>Poaceae</i> , <i>Rosaceae</i> | Reverse transcriptase-like |
| WD40 | <i>B. rapa</i> , <i>M. domestica</i> , <i>M. truncatula</i> , <i>O. sativa</i> , <i>S. bicolor</i> , <i>T. cacao</i> | <i>Brassicaceae</i> , <i>Fabaceae</i> , <i>Malvaceae</i> , <i>Poaceae</i> , <i>Rosaceae</i> | WD domain, G-beta repeat |
| zf-BED | <i>B. distachyon</i> , <i>E. grandis</i> , <i>G. max</i> , <i>H. vulgare</i> , <i>M. truncatula</i> , <i>O. sativa</i> , <i>P. trichocarpa</i> , <i>P. vulgaris</i> , <i>S. italica</i> , <i>T. aestivum</i> , <i>T. urartu</i> | <i>Fabaceae</i> , <i>Myrtaceae</i> , <i>Poaceae</i> , <i>Salicaceae</i> | BED zinc finger |
| B3 | <i>B. napus</i> , <i>B. rapa</i> , <i>F. vesca</i> , <i>H. vulgare</i> , <i>M. domestica</i> , <i>O. sativa</i> , <i>T. cacao</i> , <i>T. urartu</i> | <i>Brassicaceae</i> , <i>Malvaceae</i> , <i>Poaceae</i> , <i>Rosaceae</i> | B3 DNA-binding domain |
| NAM | <i>B. napus</i> , <i>M. domestica</i> , <i>P. trichocarpa</i> , <i>S. bicolor</i> , <i>S. italica</i> | <i>Brassicaceae</i> , <i>Poaceae</i> , <i>Rosaceae</i> , <i>Salicaceae</i> | No apical meristem (NAM) protein |
| DUF761 | <i>C. rubella</i> , <i>C. sativus</i> , <i>L. usitatissimum</i> , <i>O. sativa</i> | <i>Brassicaceae</i> , <i>Cucurbitaceae</i> , <i>Linaceae</i> , <i>Poaceae</i> | Cotton fiber-expressed protein |
| UBN2 | <i>M. domestica</i> , <i>T. cacao</i> , <i>T. urartu</i> , <i>V. vinifera</i> | <i>Malvaceae</i> , <i>Poaceae</i> , <i>Rosaceae</i> , <i>Vitaceae</i> | Gag-polypeptide of LTR copia-type |
| HMA | <i>B. napus</i> , <i>C. rubella</i> , <i>M. domestica</i> , <i>M. truncatula</i> , <i>T. urartu</i> | <i>Brassicaceae</i> , <i>Fabaceae</i> , <i>Rosaceae</i> , <i>Poaceae</i> | Heavy metal-associated domain |
| Thioredoxin | <i>B. distachyon</i> , <i>G. raimondii</i> , <i>H. vulgare</i> , <i>O. sativa</i> , <i>S. bicolor</i> , <i>S. italica</i> , <i>T. aestivum</i> , <i>T. urartu</i> , <i>V. vinifera</i> | <i>Malvaceae</i> , <i>Poaceae</i> , <i>Vitaceae</i> | Thioredoxin |
| VQ | <i>B. napus</i> , <i>B. rapa</i> , <i>C. grandiflora</i> , <i>C. rubella</i> , <i>E. salsgineum</i> , <i>F. vesca</i> , <i>M. domestica</i> , <i>O. sativa</i> , <i>T. aestivum</i> | <i>Brassicaceae</i> , <i>Poaceae</i> , <i>Rosaceae</i> | VQ motif |
| LIM | <i>A. thaliana</i> , <i>B. napus</i> , <i>M. domestica</i> , <i>M. truncatula</i> , <i>P. persica</i> | <i>Brassicaceae</i> , <i>Fabaceae</i> , <i>Rosaceae</i> | LIM domain |
| zf-RVT | <i>G. max</i> , <i>G. raimondii</i> , <i>O. sativa</i> , <i>P. vulgaris</i> , <i>T. urartu</i> | <i>Fabaceae</i> , <i>Malvaceae</i> , <i>Poaceae</i> | Zinc-binding in reverse transcriptase |
| C1_2 | <i>B. rapa</i> , <i>O. sativa</i> , <i>T. cacao</i> | <i>Brassicaceae</i> , <i>Malvaceae</i> , <i>Poaceae</i> | C1 domain |
| DUF4219 | <i>G. max</i> , <i>M. domestica</i> , <i>V. vinifera</i> | <i>Fabaceae</i> , <i>Rosaceae</i> , <i>Vitaceae</i> | Domain of unknown function (DUF4219) |
| EF_hand_5 | <i>M. domestica</i> , <i>P. trichocarpa</i> , <i>T. urartu</i> | <i>Poaceae</i> , <i>Rosaceae</i> , <i>Salicaceae</i> | EF-hand domain pair |
| Myb_DNA-binding | <i>B. distachyon</i> , <i>E. grandis</i> , <i>R. communis</i> | <i>Euphorbiaceae</i> , <i>Myrtaceae</i> , <i>Poaceae</i> | Myb-like DNA-binding domain |
| Peptidase_C48 | <i>F. vesca</i> , <i>G. max</i> , <i>Z. mays</i> | <i>Fabaceae</i> , <i>Poaceae</i> , <i>Rosaceae</i> | Ulp1 protease family, C-terminal catalytic domain |
| gag_pre-integrase | <i>M. domestica</i> , <i>T. urartu</i> , <i>V. vinifera</i> | <i>Poaceae</i> , <i>Rosaceae</i> , <i>Vitaceae</i> | GAG-pre-integrase domain |
| Integrase core | <i>T. cacao</i> , <i>T. urartu</i> , <i>V. vinifera</i> | <i>Malvaceae</i> , <i>Poaceae</i> , <i>Vitaceae</i> | Integrase core domain |
| Jacalin | <i>B. distachyon</i> , <i>E. grandis</i> , <i>H. vulgare</i> , <i>O. sativa</i> , <i>S. bicolor</i> , <i>S. italica</i> , <i>T. aestivum</i> | <i>Myrtaceae</i> , <i>Poaceae</i> | Jacalin-like lectin domain |
| DUF3633 | <i>A. thaliana</i> , <i>B. napus</i> , <i>M. domestica</i> , <i>P. persica</i> | <i>Brassicaceae</i> , <i>Rosaceae</i> | Protein of unknown function (DUF3633) |
| FNIP | <i>H. vulgare</i> , <i>M. truncatula</i> , <i>S. bicolor</i> , <i>S. italica</i> | <i>Fabaceae</i> , <i>Poaceae</i> | FNIP repeat |
| Kelch_1 | <i>B. napus</i> , <i>H. vulgare</i> , <i>T. aestivum</i> , <i>T. urartu</i> | <i>Brassicaceae</i> , <i>Poaceae</i> | Kelch motif |

Table 1 Most prevalent integrated domains in flowering plants (*Continued*)

| | | | |
|-----------------|---|----------------------------------|--|
| PP2C | <i>F. vesca, H. vulgare, T. aestivum, T. urartu</i> | <i>Poaceae, Rosaceae</i> | Protein phosphatase 2C |
| AvrRpt-cleavage | <i>H. vulgare, M. domestica, O. sativa</i> | <i>Poaceae, Rosaceae</i> | Cleavage site for pathogenic type III effector avirulence factor Avr |
| CBFB_NFYA | <i>B. napus, B. rapa, L. usitatissimum</i> | <i>Brassicaceae, Linaceae</i> | CCAAT-binding transcription factor (CBF-B/NF-YA) subunit B |
| DUF4283 | <i>F. vesca, M. domestica, M. truncatula</i> | <i>Fabaceae, Rosaceae</i> | Domain of unknown function (DUF4283) |
| F-box | <i>M. domestica, S. lycopersicum, S. tuberosum</i> | <i>Rosaceae, Solanaceae</i> | F-box domain |
| Glutaredoxin | <i>H. vulgare, S. bicolor, S. tuberosum</i> | <i>Poaceae, Solanaceae</i> | Glutaredoxin |
| PP2 | <i>S. bicolor, T. cacao, Z. mays</i> | <i>Malvaceae, Poaceae</i> | Phloem protein 2 |
| PPR_2 | <i>B. napus, F. vesca, M. domestica</i> | <i>Brassicaceae, Rosaceae</i> | PPR repeat family |
| PRK | <i>G. raimondii, P. persica, T. cacao</i> | <i>Malvaceae, Rosaceae</i> | Phosphoribulokinase/uridine kinase family |
| U-box | <i>B. napus, B. rapa, F. vesca</i> | <i>Brassicaceae, Rosaceae</i> | U-box domain |
| UBN2_3 | <i>M. domestica, T. urartu, Z. mays</i> | <i>Poaceae, Rosaceae</i> | Gag-polypeptide of LTR copia-type |
| Abhydrolase_6 | <i>M. domestica, Z. mays</i> | <i>Poaceae, Rosaceae</i> | Alpha/beta hydrolase family |
| B_lectin | <i>G. max, V. vinifera</i> | <i>Fabaceae, Vitaceae</i> | D-mannose binding lectin |
| C1_3 | <i>B. rapa, T. cacao</i> | <i>Brassicaceae, Malvaceae</i> | C1-like domain |
| Cyclin_C | <i>E. grandis, M. truncatula</i> | <i>Fabaceae, Myrtaceae</i> | Cyclin, C-terminal domain |
| Cyclin_N | <i>E. grandis, M. truncatula</i> | <i>Fabaceae, Myrtaceae</i> | Cyclin, N-terminal domain |
| DUF247 | <i>M. domestica, Z. mays</i> | <i>Poaceae, Rosaceae</i> | Plant protein of unknown function |
| FBD | <i>B. napus, M. domestica</i> | <i>Brassicaceae, Rosaceae</i> | FBD |
| Myb_DNA-bind_3 | <i>F. vesca, Z. mays</i> | <i>Poaceae, Rosaceae</i> | Myb/SANT-like DNA-binding domain |
| PA | <i>M. domestica, V. vinifera</i> | <i>Rosaceae, Vitaceae</i> | PA domain |
| PAH | <i>A. thaliana, Z. mays</i> | <i>Brassicaceae, Poaceae</i> | Paired amphipathic helix repeat |
| PARP | <i>A. lyrata, T. urartu</i> | <i>Brassicaceae, Poaceae</i> | Poly(ADP-ribose) polymerase catalytic domain |
| PPR_1 | <i>B. napus, M. domestica</i> | <i>Brassicaceae, Rosaceae</i> | PPR repeat |
| PTEN_C2 | <i>E. grandis, T. urartu</i> | <i>Myrtaceae, Poaceae</i> | C2 domain of PTEN tumour suppressor protein |
| Proteasome_A_N | <i>M. domestica, P. trichocarpa</i> | <i>Rosaceae, Salicaceae</i> | Proteasome subunit A N-terminal signature |
| RVT_2 | <i>G. max, T. cacao</i> | <i>Fabaceae, Malvaceae</i> | Reverse transcriptase (RNA-dependent DNA polymerase) |
| S_locus_glycop | <i>G. max, V. vinifera</i> | <i>Fabaceae, Vitaceae</i> | S-locus glycoprotein family |
| Sugar_tr | <i>B. rapa, M. domestica</i> | <i>Brassicaceae, Rosaceae</i> | Sugar (and other) transporter |
| TPR_11 | <i>P. patens, T. cacao</i> | <i>Funariaceae, Malvaceae</i> | TPR repeat |
| TPR_12 | <i>C. subellipsoidea, V. carteri</i> | <i>Coccomyaceae, Volvocaceae</i> | Tetratricopeptide repeat |
| UPF0114 | <i>L. usitatissimum, M. truncatula</i> | <i>Fabaceae, Linaceae</i> | Uncharacterized protein family, UPF0114 |
| XH | <i>B. rapa, T. urartu</i> | <i>Brassicaceae, Poaceae</i> | XH domain |
| zf-CCHC_4 | <i>F. vesca, T. urartu</i> | <i>Poaceae, Rosaceae</i> | Zinc knuckle |
| zf-RING_2 | <i>F. vesca, T. aestivum</i> | <i>Poaceae, Rosaceae</i> | Ring finger domain |

^aIntegrated domains present across at least two plant families. Additional file 3 contains the full list of integrated domains. Additional file 6 contains list of domains for each protein

Additional files 2, 3, 6 and 7). The only plant with no NLR-IDs was papaya (*C. papaya*), which has a low number of 58 NLRs in total. Despite variability in the total number of NLRs across flowering plants, on average in each species NLR-IDs represented about 10 % of all NLRs and correlated with increases and decreases in total NLR numbers among species. There is a substantial variation in the number of NLRs and their integrated domains across flowering plants. However, it is hard to conclude whether there are significant differences in fusion rates across different lineages as our analyses are based on current proteome predictions for each species that may have missed or miss-annotated genes.

We have used publicly available RNA-seq data to further test which of the predicted fusions are supported by the expression evidence in two newly sequenced crop species, *B. rapa* and bread wheat, *T. aestivum*. Manual examination of RNA-seq alignments showed that in *B. rapa* 20 out of 25 genes were expressed and only 8 genes (40 %) had reads spanning exons connecting the predicted NLR and its ID (Additional files 10 and 11). In *T. aestivum*, 25 out of 43 genes showed strong expression, and 20 out of 25 (80 %) of the expressed fusions were strongly supported by RNA-seq reads (Additional file 12). For wheat (*T. aestivum* and *T. urartu*), we have confirmed four NLR-IDs by amplification from cDNA and sub-cloning (Additional file 13). As these are examples of the draft genome sequences, our manual analyses confirm that many of the detected fusions are real and not due to miss-assembly or annotation errors, although more experimental evidence is needed to test all predictions.

We used Fisher's exact test to see if the detected protein domains are overrepresented in NLR-IDs compared to the rest of the genomes (Additional file 14). We observed that indeed most of the domains have a significant association with the NLR-ID set (P value <0.05). However, the integration event by itself does not signify functional relevance. Therefore, we tested which of the fused domains are found throughout several plant families, which could indicate either recurrent integration or retention of ancient fusions.

Re-occurring and ancient domain integrations

Overall, we found 265 distinct integrated domains in 750 NLR proteins. Comparing NLR-IDs across species, we observed that 61 distinct Pfam domains are present in plants belonging to at least two different families. These prevalent domains are enriched in protein activities associated with protein kinases, DNA-binding domains and protein-protein interactions (Fig. 2, Table 1).

Domains associated with retrotransposons are also found in fusion with NLRs ubiquitously across plants (Fig. 2, Table 1). Retrotransposons have been shown to have a role in R-gene diversity and function [57], yet currently we do not have enough evidence to suggest transposon activity plays a role in generating NLR-IDs.

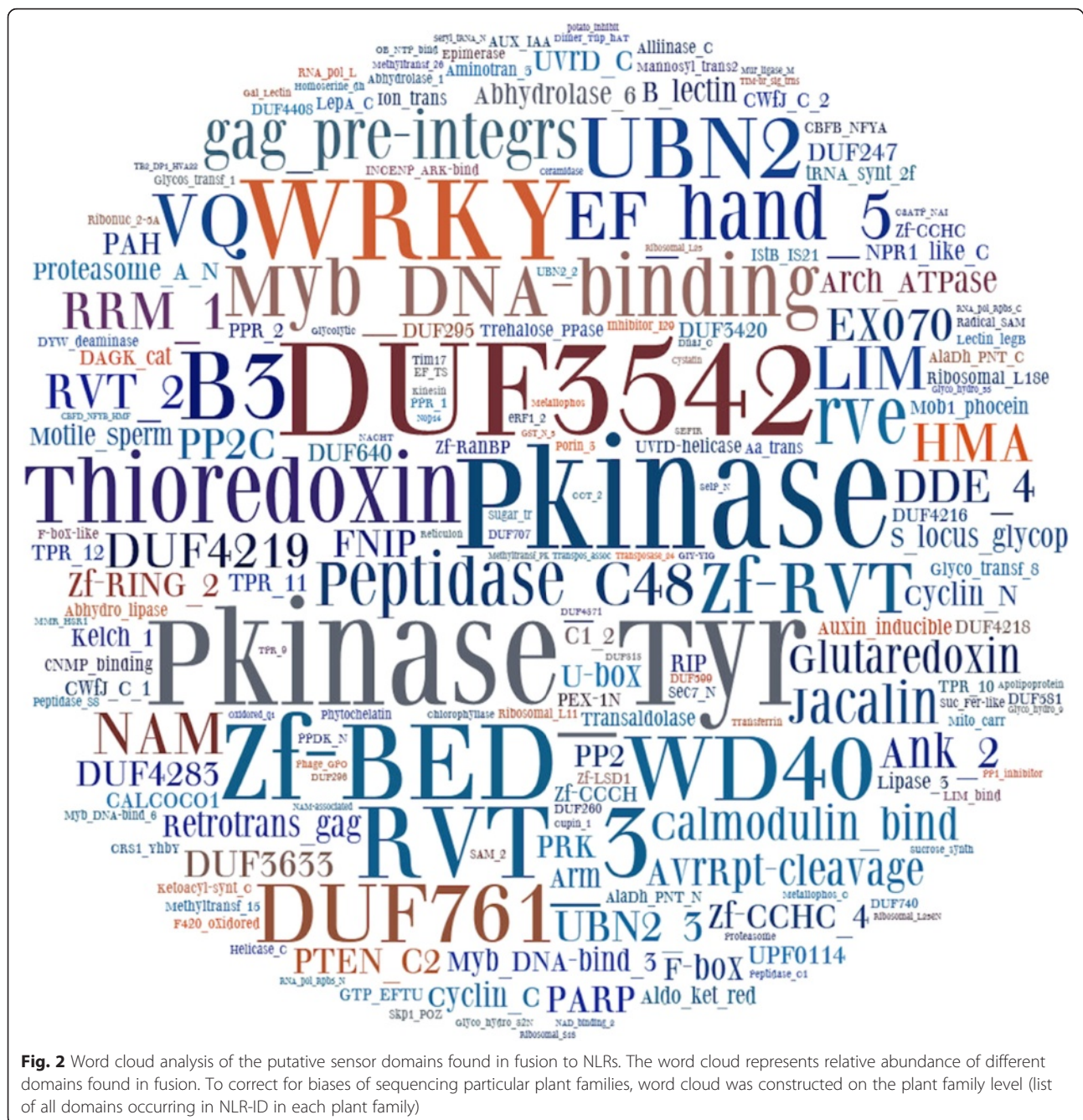
While some domains showed clear recurrent integration (i.e. WRKYs, see detailed analyses in a later section), a few proteins suggested ancient integration events. For example, an NLR-jacalin fusion is present in 6 out of 8 grasses and we confirmed this fusion by sub-cloning from cDNA of *T. aestivum*. As the grasses (*Poaceae*) separated from a common ancestor 70–55 million years ago [58], the NLR-jacalin is likely to be an ancient fusion event. Another validated fusion, NLR-Exo70 is present in two analyzed wheat species as well as barley, but functions as separate proteins in rice. Therefore, the NLR-Exo70 fusion event likely occurred at the split between *Triticeae* and *Oryza*, 40 million years ago.

Together, the results show that NLR-IDs are present in the genomes of most flowering plants, and we could detect that at least 61 integrated domains were selected by more than one plant family. These data suggest that plants share a common mechanism of NLR evolution through gene fusions. We hypothesize that these newly integrated domains serve as baits for the pathogen and that the same pathways are targeted across multiple plant species.

Integrated domains overlap with host targets of pathogen effectors

Several studies set out to reveal host targets of phyto-pathogen effectors by conducting genome-wide effector interactome screens, such as yeast two-hybrid screens against Arabidopsis proteins [47, 48]. We examined the overlap between protein domains fused to plant NLRs and protein domains found to interact with effectors. To ensure uniform analyses, we annotated domains of the predicted effector targets using our pipeline. We found that 41 out of 213 domains that are found in the Arabidopsis interactome studies are also present in NLR-IDs (Fig. 3a, Table 2). Overlapping domains include protein kinases, DNA-binding and transcription factor proteins, and proteins involved in redox reactions as well as hormone signaling and cytoskeleton (Fig. 3a, Table 2).

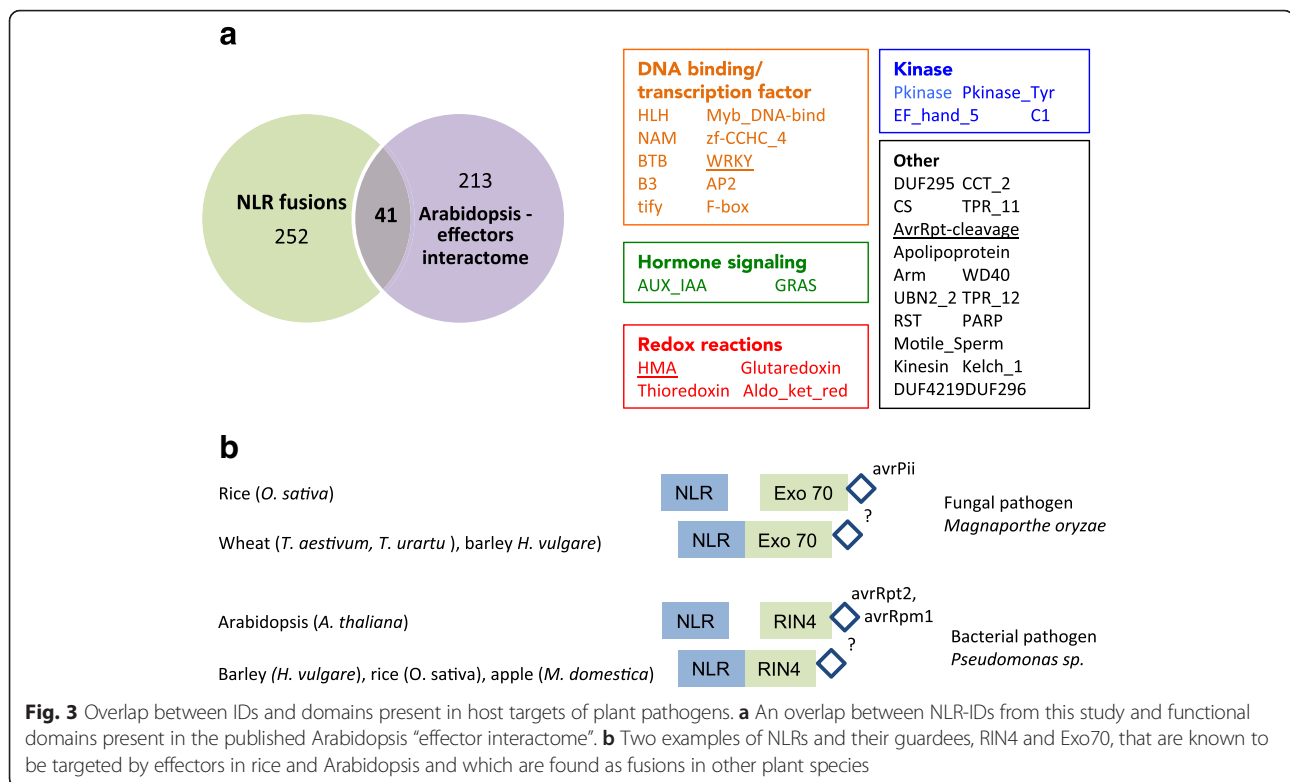
A random protein set sampled from all plant proteomes could have domains in common with the Arabidopsis interactome. Some domains, such as protein kinases and Myb family DNA-binding domains, are indeed prevalent in plant genomes, and using 5 % confidence intervals, we cannot exclude a possibility of a random overlap. However, for the majority of domains, we find a significant overlap between effector targets and domains in fusions (P <0.05) (Additional file 14).



Overall, this strong overlap indicates that protein domains fused to NLRs could be effector targets. Conceivably, effector targets not detected in our survey could occur as fusions in as yet uncharacterized plant species or sub-species. Future effector interactome screens are needed to test the identified NLR-IDs.

Overlap of IDs with effector targets is further exemplified by presence of well-characterized guardees on our fusions list. A recently found interaction between rice

blast (*M. oryzae*) effector AvrPii and rice exocyst complex factor Exo70 is in line with our finding of an NLR-Exo70 fusion in wheat (Fig. 3b, Table 1). Wheat blast also caused by variants of the *M. oryzae* species might be harboring an effector recognized by this fusion. Alternatively, NLR-Exo70 in wheat might be the basis for host specificity of the rice blast pathogen. One of the most studied effector targets, RIN4, which interacts with several NLRs, including RPS2 and RPM1 in a classic



guard/guardee system, is found as an NLR-RIN4 fusion in several species, including barley, rice and apple (Fig. 3b, Tables 1 and 2). These findings further support the links between guardees and integrated sensor domain models, in which a fusion reveals a previously interacting NLR and guardee that are now also linked together genetically.

NLR-integrated kinase domains are frequent and intact

The most abundant class of NLR-fusion is the protein kinase domain found as early as in mosses and in 161 NLR proteins across 19 species and 8 plant families (Fig. 4a, Table 1). Both serine and tyrosine kinases are present, either as amino-terminal or carboxyl-terminal fusions (Additional files 6 and 8). A class of kinases called non-RD kinases are known to function in the immune pathways in both plants and mammals and are also often found in the receptor-like kinases that transduce PAMP-triggered immunity [59]. We examined the kinase motifs in NLR-IDs and observed that both RD and non-RD kinases are present.

Interestingly, a protein kinase was associated with another domain fusion in 14 different combinations (Fig. 4b). Some domain combinations are known modifiers of protein kinase activity; for example, the kinase + EF_hand is diagnostic of a Ca²⁺-dependent protein kinase that was part of a single gene before fusion with NLR. Other combinations likely represent sequential

fusion events, such as a kinase-NLR-NPR1 fusion in *T. urartu* or an NLR-kinase-WRKY fusion in *A. thaliana* (Fig. 4b). There could be two explanations for such complex fusions. The kinase domains in the fusions would act as “sensors” for the effectors and double fusions would be simple stacks of different sensor domains. Alternatively, the kinases represent a class of signaling domains recruited by NLRs and the additional domains are operative enzymes that function as “integrated” sensors. Given the examples of PBS1 and Pto, two protein kinases that are guardees, it is most likely that the former hypothesis is true and that at least some of the kinase fusions are integrated sensors for the effectors.

The current integrated decoy model suggests that the fused proteins might lose their biochemical activity after integration while retaining effector-binding properties [25]. To test whether NLR-kinase fusions follow the current model of integrated decoy, we have tested whether the kinase activity is likely to be conserved. After aligning all kinase regions from NLR-IDs, we examined conservation of active site region and catalytic residues. We explored sequence conservation by mapping alignment of all kinases found in NLRs on the 3D structural model of the kinase, with the active site conserved (red) while most of the other regions are variable (blue) (Fig. 5b). The catalytic lysine and aspartate are also conserved in all kinases as can be seen from the

Table 2 Pathogenic effectors, their previously identified interacting Arabidopsis proteins and corresponding domains that were also detected in NLR-IDs

| Effector | Interacting Arabidopsis gene | Common domain with NLR-ID | Domain description |
|-------------------|------------------------------|---------------------------|--|
| OEC55 | AT1G04690 | Aldo_ket_red | Aldo/keto reductase family |
| ATR1_group | AT4G00980 | DUF4219 | Domain of unknown function (DUF4219) |
| ATR1_group | AT4G00980 | UBN2_2 | Gag-polypeptide of LTR copia-type |
| ATR1_group | AT4G00980 | zf-CCHC_4 | Zinc knuckle |
| ATR13_group | AT5G66560 | BTB | BTB/POZ domain |
| ATR13_group | AT5G52750 | HMA | Heavy metal-associated domain |
| avrB_group | AT3G25070 | AvrRpt-cleavage | Cleavage site for pathogenic type III effector avirulence factor Avr |
| avrB_group | AT1G14920 | GRAS | GRAS domain family |
| avrB_group | AT2G47060 | Pkinase | Protein kinase domain |
| avrB_group | AT3G17410 | Pkinase_Tyr | Protein tyrosine kinase |
| avrC_group | AT4G17680 | Apolipoprotein | Apolipoprotein A1/A4/E domain |
| avrPto_group | AT5G22355 | C1_2 | C1 domain |
| avrPto_group | AT5G22355 | C1_3 | C1-like domain |
| avrPto_group | AT4G11890 | Pkinase | Protein kinase domain |
| avrPto_group | AT3G48150 | TPR_11 | TPR repeat |
| AvrRps4_Pph_1448A | AT4G11070 | WRKY | WRKY DNA-binding domain |
| AVRRPT2_group | AT4G00710 | Pkinase_Tyr | Protein tyrosine kinase |
| AVRRPT2_group | AT4G00710 | TPR_11 | TPR repeat |
| HARXL10_WACO9 | AT1G50420 | GRAS | GRAS domain family |
| HARXL106_group | AT1G09270 | Arm | Armadillo/beta-catenin-like repeat |
| HARXL106_group | AT4G02150 | Arm | Armadillo/beta-catenin-like repeat |
| HARXL106_group | AT1G32230 | PARP | Poly(ADP-ribose) polymerase catalytic domain |
| HARXL106_group | AT1G32230 | RST | RCD1-SRO-TAF4 (RST) plant domain |
| HARXL14 | AT5G66200 | Arm | Armadillo/beta-catenin-like repeat |
| HARXL149 | AT4G35580 | NAM | No apical meristem (NAM) protein |
| HARXL16 | AT1G18400 | HLH | Helix-loop-helix DNA-binding domain |
| HARXL16 | AT4G32570 | tify | tify domain |
| HARXL21 | AT1G15750 | WD40 | WD domain, G-beta repeat |
| HARXL44 | AT4G25920 | DUF295 | Protein of unknown function (DUF295) |
| HARXL44 | AT4G16380 | HMA | Heavy metal-associated domain |
| HARXL45_group | AT4G02550 | Myb_DNA-bind_3 | Myb/SANT-like DNA-binding domain |
| HARXL68 | AT1G45145 | Thioredoxin | Thioredoxin |
| HARXL68 | AT5G42980 | Thioredoxin | Thioredoxin |
| HARXL73 | AT4G39050 | Kinesin | Kinesin motor domain |
| HARXL79 | AT5G56950 | NAP | Nucleosome assembly protein (NAP) |
| HARXLL445_group | AT2G35500 | CS | CS domain |
| HARXLL470_WACO9 | AT5G49000 | F-box | F-box domain |
| HARXLL470_WACO9 | AT5G49000 | Kelch_1 | Kelch motif |
| HARXLL470_WACO9 | AT1G79430 | Myb_DNA-binding | Myb-like DNA-binding domain |
| HARXLL492 | AT3G60600 | Motile_Sperm | Major sperm protein (MSP) domain |
| HARXLL60 | AT2G23290 | Myb_DNA-bind_6 | Myb-like DNA-binding domain |
| HARXLL73_group | AT1G03960 | EF_hand_5 | EF-hand domain pair |
| HARXLL73_group | AT4G26110 | NAP | Nucleosome assembly protein (NAP) |

Table 2 Pathogenic effectors, their previously identified interacting *Arabidopsis* proteins and corresponding domains that were also detected in NLR-IDs (*Continued*)

| | | | |
|--------------------|-----------|-----------------|-------------------------------------|
| HARXLL73_group | AT5G56290 | TPR_11 | TPR repeat |
| HOPAB_group | AT3G57720 | Pkinase | Protein kinase domain |
| HOPAB_group | AT3G46370 | Pkinase_Tyr | Protein tyrosine kinase |
| HOPAB_group | AT3G27960 | TPR_12 | Tetratricopeptide repeat |
| HopBB1_Pmo_M301020 | AT3G17860 | CCT_2 | Divergent CCT motif |
| HopBB1_Pmo_M301020 | AT3G17860 | tify | tify domain |
| HOPD1_group | AT5G22290 | NAM | No apical meristem (NAM) protein |
| HOPF_group | AT2G04740 | BTB | BTB/POZ domain |
| HOPH1_group | AT5G43700 | AUX_IAA | AUX/IAA family |
| HopP1_Pto_DC3000 | AT4G36540 | HLH | Helix-loop-helix DNA-binding domain |
| HOPR1_group | AT5G60120 | AP2 | AP2 domain |
| HopX_group | AT5G13810 | Glutaredoxin | Glutaredoxin |
| OEC115 | AT4G28640 | AUX_IAA | AUX/IAA family |
| OEC115 | AT5G08130 | HLH | Helix-loop-helix DNA-binding domain |
| OEC115 | AT3G21490 | HMA | Heavy metal-associated domain |
| OEC115 | AT3G10480 | NAM | No apical meristem (NAM) protein |
| OEC45 | AT1G63480 | DUF296 | Domain of unknown function (DUF296) |
| OEC45 | AT4G00120 | HLH | Helix-loop-helix DNA-binding domain |
| OEC45 | AT1G12520 | HMA | Heavy metal-associated domain |
| OEC45 | AT3G22420 | Pkinase | Protein kinase domain |
| OEC59 | AT4G08320 | TPR_11 | TPR repeat |
| OEC67 | AT1G25550 | Myb_DNA-binding | Myb-like DNA-binding domain |
| OEC78 | AT4G30080 | AUX_IAA | AUX/IAA family |
| OEC78 | AT4G30080 | B3 | B3 DNA-binding domain |
| OEC78 | AT4G02590 | HLH | Helix-loop-helix DNA-binding domain |

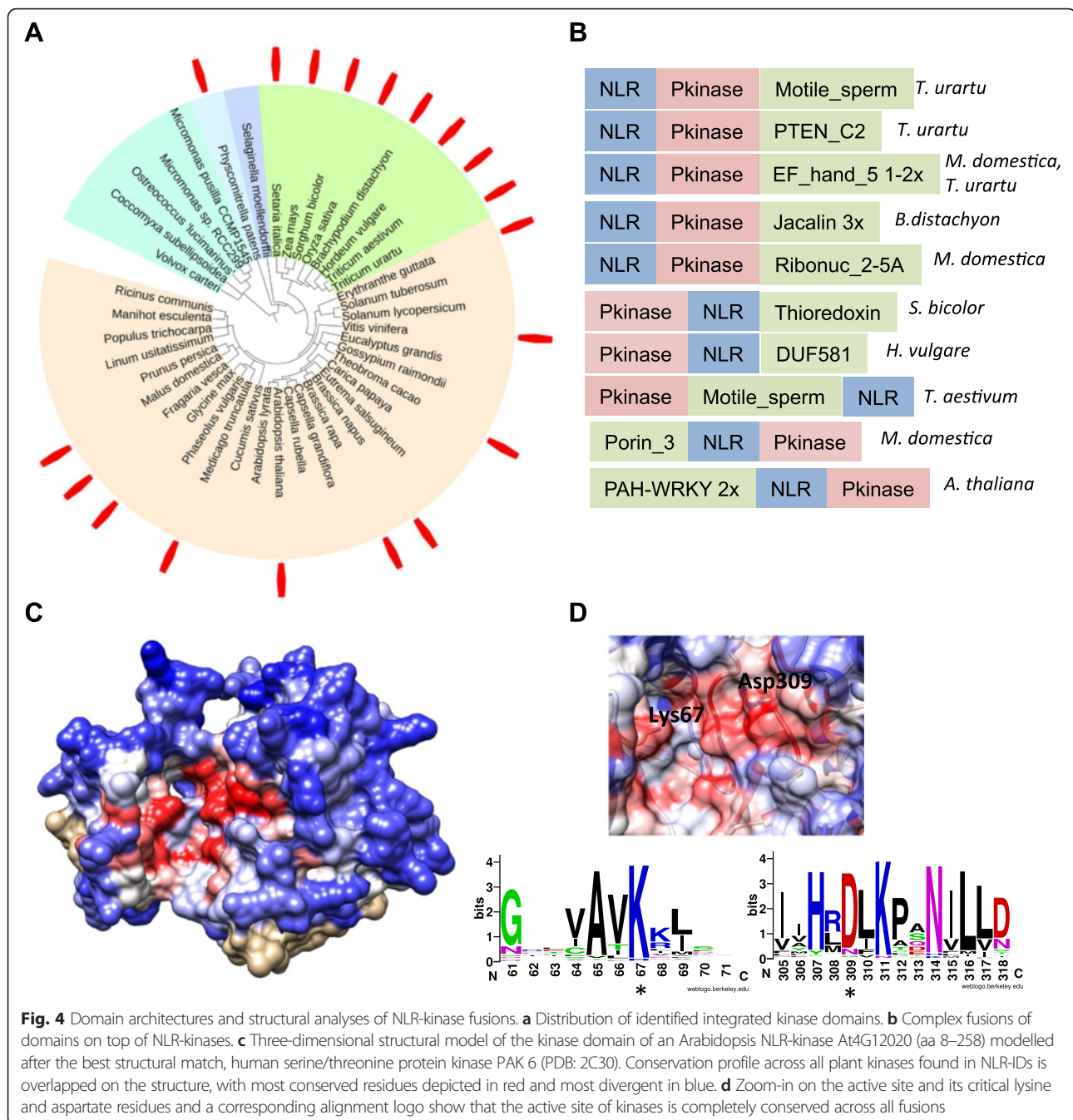
structure as well as alignment consensus logo (Fig. 5c). Overall, these data indicate that the kinases fused with NLRs encode intact full-length kinase domains that are potentially catalytically active.

WRKY transcription factor integration into NLRs occurred independently in several lineages of plants

The WRKY family of transcription factors is large and its members can be positive or negative regulators of both PTI and ETI [3], or in other plant signaling networks. In *Arabidopsis*, more than 70 % of WRKY genes are responsive to pathogen infection and salicylic acid treatment [60, 61], suggesting a major role of these proteins in plant defense. We have found the WRKY domain to be present in 35 NLR-ID genes from 13 plant species, in monocots and dicots, including previously reported *A. thaliana*, *A. lyrata*, *Fragaria vesca*, *Capsella rubella*, *Glycine max*, *Theobroma cacao*, *Sorghum bicolor*, *Setaria italica*, *O. sativa* [62] as well as in *M. domestica*, *Conradina grandiflora*, *B. distachyon*, *Hordeum vulgare*, *T. aestivum* and *T. urartu* (Table 1,

Additional file 15). Similar to Rinerson et al. [62], we also detected an NLR-WRKY fusion in *Panicum virgatum*, but did not include it in our high-throughput analyses due to current restrictions on using genome-wide data for this species. The only reported NLR-WRKY that was not found in our screen is GrWRKY1 from *Gossypium raimondii*, which is according to the authors of the study “truncated and difficult to classify” [62].

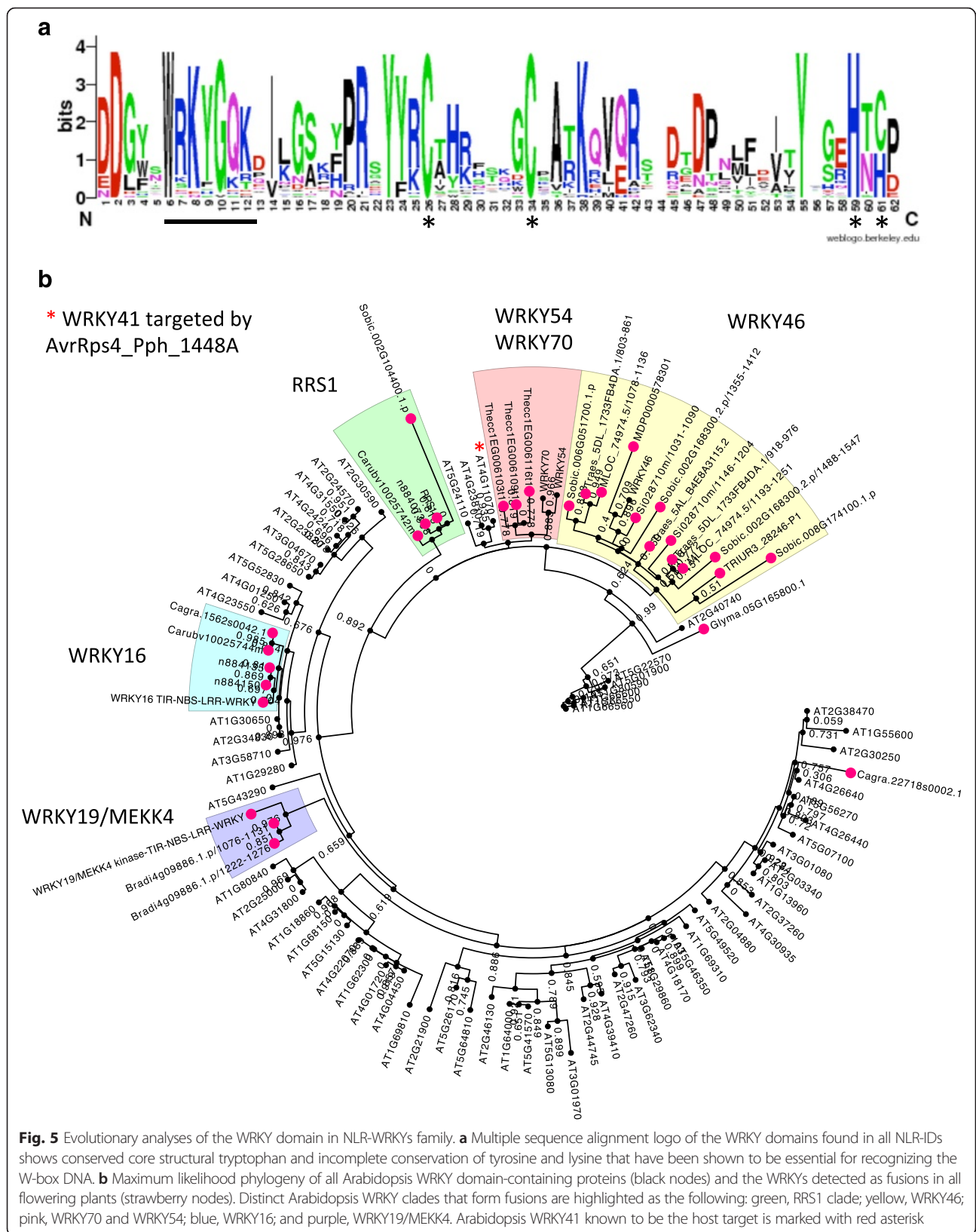
Our protein sequence alignment of 7 domain regions from NLR-IDs showed that all sequences contain functional Zn²⁺-binding motifs CX₄₋₅CX₂₂₋₂₃HXH or CX₇CX₂₃HXC (Fig. 5a). While the protein core stabilizing tryptophan is conserved, the DNA-binding motif of WRKYG[Q/K]K is mutated in several fusion proteins (Fig. 5a), including variants of the tyrosine and lysine that have been shown to be essential for recognizing the W-box DNA element [63]. The group I WRKY NLR-fusion proteins, which contain 2 × WRKY motifs, often show mutations in the second critical motif. Given this evidence, we cannot exclude that in



several NLR-IDs, WRKY region is indeed a “decoy” protein deficient in its DNA-binding activity.

Our data also support that the NLR-WRKY fusions occurred independently in several lineages, including both monocots and dicots. The phylogenetic analyses of all fused WRKY domains together with all WRKY proteins from Arabidopsis showed that fusions arose at least five times and involved homologs of RRS1, WRKY16, WRKY19, WRKY46 and WRKY54/70 (Fig. 5b, Additional file 16). Interestingly, the WRKY46 fusion appears to be specific to

monocots, but it is widespread and potentially an old fusion event as it is present in wheat (*T. aestivum* and *T. urartu*), barley (*H. vulgare*), sorghum (*S. bicolor*) and *S. italica*. It has been reported that WRKY46 plays a role in basal resistance against bacterial pathogens and is specifically induced by salicylic acid [60, 64, 65], and is therefore a plausible pathogen target. The WRKY54/70 cluster together with the NLR-WRKY fusions in *T. cacao*, and in Arabidopsis they have been implicated in resistance as a WRKY54/70 double mutant shows increased susceptibility to *Pseudomonas*



infection [66]. Next to the WRKY54/70 is the WRKY41 (Fig. 5b), which is targeted by a number of bacterial effectors in the Arabidopsis interactome yeast two-hybrid screen (Table 2). Finally, WRKY19 (also known as MEKK4) represents a complex WRKY-NLR-kinase fusion and the clustering with similar NLR-IDs in *Brachypodium* points at a common “fusion” of immunity genes across both dicots and monocots.

This example of WRKY transcription factor family fusions across plants exemplifies recurrent fusions of the same protein family members across different lineages. It is clear that some of the fusions are more commonly found in monocots (i.e. WRKY46) while others are spread across phyla and point to the common convergent targets of pathogens infecting diverse evolutionary hosts. While most WRKYs in fusions have all the signatures of the functional WRKY transcription factors, gradual loss of activity in the “decoys” cannot be rejected as some of the integrated WRKY proteins show loss of the conserved critical residues.

Conclusions

Interaction of the effectors with fusion domains in NB-LRRs for both Arabidopsis RPS4/RRS1 and rice Pik-1, RGA4/RGA5, represented the first evidence for the “integrated decoy/sensor” pathogen recognition model, whereby the atypical domain acts as bait/trap for effector perception. Our findings of other protein domains fused to NB-LRR proteins in various plant genomes provide a new perspective on effector targets and the nature of pathogenicity. As we found NLR-IDs in most plant species, we can predict that pathogen recognition through “integrated decoy/sensor” receptors is an evolutionarily conserved mechanism of NLR diversification in flowering plants.

Overlap between fusions and effector targets point to the multiple levels of information encoded in NLR-IDs (Fig. 6). Presented NLR-IDs are likely to be molecular sensors of the effectors, so they can also be exploited to identify and validate pathogen-derived virulence factors. For many pathogens, researchers have now accumulated long lists of predicted effector molecules that are likely to be secreted or translocated inside plant cells. Systematic analyses of these effectors against the NLR-IDs in

either proteomic or yeast two-hybrid assays would allow for prioritization and validation of pathogen effectors. These validation tools represent an important milestone for deciphering pathogen arsenals and identifying new sources of disease resistance.

Extrapolating from the known mechanistic analyses, we predict that the NLR-IDs reveal not only disease resistance genes that use baits for catching the pathogen, but also potentially previously unknown effector targets inside the host. Therefore, investigation of identified fusions and tracing their origin will significantly contribute to the identification of host “susceptibility” genes.

In the future, it would be important to continue examining NLR-IDs both across plants and within each plant family to enrich our knowledge of the evolutionary history of NLR proteins. We need to understand the mechanisms leading to fusion events, and how often fusions occur in different plant lineages and across NLR families. It appears that polyploidization and ancient polyploidization played a major role in expanding the number of NLRs and consequently the number of NLR-IDs. It would be important to test if there are any genetic or molecular signatures that enable NLR platforms to be more prone to tolerating new fusions. This information will give us a better understanding of how plant immune receptors evolve to withstand pathogen pressure and can lead to new ways of engineering disease resistance.

Methods

Phylogeny of plant species

Phylogeny of all plant species was constructed using PhyloT program (<http://phylot.biobyte.de/>), using NCBI taxonomy identification numbers for each species and visualized with iTOL program. Polyploidization and ancient polyploidization events were inferred from Jiao et al. [50] and Adams et al. [51] as well as the CoGe database (https://genomeevolution.org/wiki/index.php/Plant_paleopolyploidy).

Domain annotations and high-throughput identification of gene fusions

Domain annotations in all species were performed on the currently available proteome predictions, which

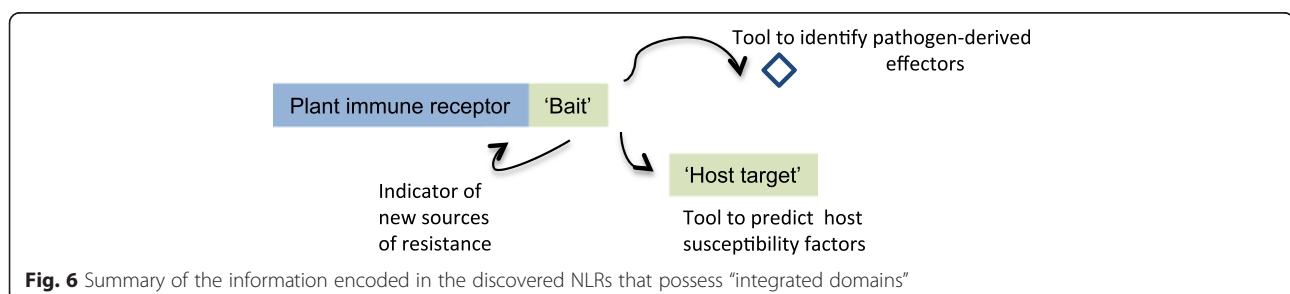


Fig. 6 Summary of the information encoded in the discovered NLRs that possess “integrated domains”

included Phytozome v10 genomes [67] available for analyses without restrictions as well as recently published wheat, barley and brassica datasets (Additional file 1). Proteins from each species were passed through uniform Pfam [68] domain identification pipeline based on the run_pfam.pl script distributed together with *PfamScan* software (HMMER2.0 package [69], e-value cutoff 1e-3). Resulting annotations were parsed using K-parse_Pfam_domains_v3.1.pl script generated in this study and available from GitHub (https://github.com/krasileva/plant_rgenes). Only highest scoring non-overlapping domains were retained for each protein. Proteins containing NB-ARC domains were extracted and checked for additional fused domains with K-parse_Pfam_domains_NLR-fusions-v2.2.pl (https://github.com/krasileva/plant_rgenes).

After filtering out classic NLR domains, such as TIR (PF01582), TIR2 (PF13676), LRR (CL0022) and RPW8 (PF05659), all other domains were considered for further analyses and a summary table of domains found in each plant species and each plant family was generated. To test for significance of overrepresentation of each domain in the fusion set, we applied the hypergeometric Fisher's exact test as implemented in K-parse_Pfam_domains_NLR-fusions-v1.0.pl (https://github.com/krasileva/plant_rgenes). Fusions in four distinct plant clades, including brassica, tomato, wheat and soybean, were manually curated using manual selection and screening of all the annotated, predicted and not predicted NB-LRRs from each species using the HMMER, SMART and BLASTP online programs (Additional file 8) showing less than 10 % of false positives in our high-throughput analyses.

In order to determine the expression of and provide an evidence for the predicted NLR-IDs, we obtained RNA-seq reads derived from 9-day-old seedlings of *B. rapa* cv. Chiifu (DRX012760/BioSample: SAMD00003761) as well as RNA-seq from leaf samples from *T. aestivum* cv. Chinese Spring (sample: ERS399938). For *B. rapa*, the reads were then aligned back to NLR-fusion genes using TOPHAT 2.1.0 [70]. For *T. aestivum* analyses, the reads were aligned back to the full genome [53] using TOPHAT 2.1.0 [70]. All alignments were performed with `-r 300 -mate-std-dev = 20`; the rest of the parameters at default values. The alignments in BAM format were then used to visualize with the Integrated Genomics Viewer (IGV) tool [71] or Tablet [72]. We then manually analyzed the splice junctions and their correspondence with the predicted gene structures as well as reads spanning exons coding for predicted protein domains, particularly the fusions.

Word cloud

Prevalence of domain fusions across plant families (each domain counted only once per family) was visualized as a word cloud at <http://www.tagxedo.com/>

with the following non-default parameters that preserve exact names of all domains: punctuation, yes; numbers, yes; remove common words, no; and combine related words, no.

Calculating overlap with interactome datasets

Amino acid sequences of the proteins reported as effector interactors [47] were annotated using the same Pfam annotation pipeline as above. The overlap of domains co-occurring in the interactors and protein fusions were manually examined. The statistical significance of the enrichment of the domains was tested using the hypergeometric Fisher's exact test, which tested for significance of overrepresentation of each domain in the fusion set and implemented in K-parse_Pfam_domains_NLR-fusions-v1.0.pl (https://github.com/krasileva/plant_rgenes).

Protein family sequence alignment, structural modeling and phylogenetic analyses

For each protein family of interest, the amino acid sequences of all fusion-containing proteins were extracted using K-get_fasta_from_ids.pl and aligned together on the corresponding Pfam HMM profile using the *hmmalign* program (HMMER2.0) [69]. The alignment was converted from Stockholm to FASTA format using bioscripts.convert tools v0.4 (<https://pypi.python.org/pypi/bioscripts.-convert/0.4>). The alignment was examined with Belu program and trimmed to the domain borders. Trimmed sequences were then re-aligned with MUSCLE [73].

The evolution of TIR₂ domains was inferred with MEGA5 [74] using the maximum likelihood method based on the Poisson correction model [75]. The bootstrap consensus tree was inferred from 400 bootstrap replicates [76]. Initial tree(s) for the heuristic search were obtained automatically as follows: when the number of common sites was <100 or less than one-fourth of the total number of sites, the maximum parsimony method was used; otherwise BIONJ method with MCL distance matrix was used. The tree was drawn to scale, with branch lengths measured in the number of substitutions per site. The analysis involved 74 amino acid sequences. All positions were evaluated regardless of alignment gaps, missing data and ambiguous bases. There were a total of 75 positions in the final dataset.

Structural modelling of the kinase domain was performed with Phyre2 using amino acid sequence of the kinase domain from At4G12020 (aa 8–258) and the best structure (highest percent identity, most sequence coverage) modelled after human serine/threonine protein kinase PAK 6 (PDB: 2C30) was picked as a template. The structure was visualized in Chimera [77] and amino acid conservation from multiple sequence alignment of all kinase fusions was mapped to the structure using “render by conservation” function with 0.017 and 0.85 conservation

cutoffs. The alignment logo of the kinase active site was constructed with WebLogo (weblogo.berkeley.edu/logo.cgi). The phylogeny of WRKY transcription factors was constructed with PhyML method using Phylogeny.fr with SH-like approximate likelihood ratio test. The tree was annotated and visualized using FigTree v1.4.2 (<http://tree.bio.ed.ac.uk/software/figtree/>). WRKY alignment conservation logo plot was constructed with WebLogo.

Availability of supporting data

The plant proteome datasets analyzed in this study were obtained from publicly available databases Phytozome v10 and Ensembl Plants, and are listed in Additional file 1. Specific sequences of NLR and NLR-ID proteins and corresponding domain architectures are available in Additional files 2, 3, 4, 5 and 7. All scripts written for this study are available from GitHub at https://github.com/krasileva/plant_rgenes. All additional files are supplied in standard formats (Excel, PDF and FASTA [in Unix line break format]). In the event that any additional file is not compatible for a user computer's platform, please contact corresponding author: Ksenia.Krasileva@tgac.ac.uk.

Additional files

Additional file 1: Plant datasets used in this study. A table with the description of species, genome builds and databases from where they were retrieved. (XLSX 32 kb)

Additional file 2: NLR and NLR-ID architectures detected in each species. (XLSX 44 kb)

Additional file 3: Summary of the integrated domains and their prevalence. (XLSX 58 kb)

Additional file 4: Protein ids and corresponding domains of putative NLRs from all plant species. A table of domain architectures detected in all NB-ARC-containing proteins. (XLSX 953 kb)

Additional file 5: Amino acid FASTA sequences of all putative NLRs. Unix-encoded plain text file with FASTA sequences for all NB-ARC-containing proteins from Additional file 4. (TXT 14163 kb)

Additional file 6: Protein ids and corresponding domains of putative NLR-IDs from all plant species. Table of domain architectures detected in each protein classified as NLR-fusion. (XLSX 114 kb)

Additional file 7: Amino acid FASTA sequences of putative NLR-IDs. Unix-encoded plain text file with FASTA sequences for all NLR-fusion proteins from Additional file 6. (TXT 917 kb)

Additional file 8: Manual verification of domains predicted by high-throughput scripts with webservers for brassica, tomato, wheat and soybean. (XLSX 22 kb)

Additional file 9: Phylogeny of TIR2 proteins from plants and phytopathogenic bacteria. (PDF 447 kb)

Additional file 10: *B. rapa* fusion validation by RNA-seq. Summary of manual validation of *B. rapa* NLR-IDs using RNA-seq data. (XLSX 36 kb)

Additional file 11: Visual examples of validated *B. rapa* fusions. (PDF 375 kb)

Additional file 12: *T. aestivum* fusion validation by RNA-seq. Summary of manual validation of *T. aestivum* NLR-IDs using RNA-seq data. (XLSX 60 kb)

Additional file 13: Cloned *T. aestivum* and *T. urartu* fusions. Summary of *T. aestivum* and *T. urartu* fusions confirmed by sub-cloning from cDNA. (XLSX 23 kb)

Additional file 14: Enrichment analyses of NLR-IDs. Summary of hypergeometric tests for each domain present in NLR-IDs in each plant species. (XLSX 84 kb)

Additional file 15: Visual representation of distribution of WRKY fusions across flowering plants. (PDF 1729 kb)

Additional file 16: Maximum likelihood phylogenetic tree of WRKY transcription factors in fusion with NLRs in all plants together with all other *Arabidopsis* WRKY proteins. (TXT 4 kb)

Abbreviations

CC: coiled coil; ETI: effector-triggered immunity; HMA: heavy metal-associated; ID: integrated domain; LRR: leucine-rich repeats; NB: nucleotide-binding; NCBI: National Center for Biotechnology Information; NLR: nucleotide-binding leucine-rich repeat; PAMP: pathogen-associated microbial pattern; PTI: PAMP-triggered immunity; TIR: Toll/interleukin-1 receptor/resistance protein.

Competing interests

The authors declare that they have no competing interests.

Authors' contributions

KVK, PFS, VC and JJ conceived and designed this study. KVK wrote the scripts, performed high-throughput domain annotation analyses, hypergeometric tests, as well as specific analyses of the kinase domains and WRKY phylogeny. PFS carried out the manual analyses of NLRs from selected plant families and TIR2 domain analyses in phytopathogenic bacteria. VC analyzed overlaps between NLR-IDs and host proteins targeted by effectors. VC, KVK and GD performed validation of NLR-IDs from RNA-seq data and gene cloning from cDNA samples. All authors contributed significantly to data analyses, discussion of results and preparation of this manuscript. All authors read and approved the final manuscript.

Acknowledgements

Authors are grateful to Wiktor Jurkowski, Luca Venturini, Dina Raats, Sophien Kamoun, Ben Petre and Daniil Prigozhin for insightful comments and suggestions; Hans Vasquez-Gross for tips on downloading Phytozome database; The Sainsbury Laboratory (TSL) support groups for technical assistance; and to all TSL and The Genome Analysis Centre (TGAC) staff for providing thoughtful comments during seminars. This research was supported in part by the NBI Computing infrastructure for Science (CiS) group through access to high performance computing. KVK is strategically supported by the Biotechnology and Biological Science Research Council (BBSRC) and the Gatsby Charitable Foundation. JJ and PFS are supported by BBSRC grant BB/M008193/1 and PFS is supported by the EC FP7-PEOPLE-2011-IEF Intra-European Fellowships (299621). JJ and VC receive additional support from BBSRC/DBT grant BB/L011646/1.

Author details

¹The Sainsbury Laboratory, Norwich Research Park, Norwich, UK. ²The Genome Analysis Centre, Norwich Research Park, Norwich, UK. ³Division of Plant and Microbial Sciences, School of Biosciences, University of Exeter, Exeter, UK.

Received: 12 October 2015 Accepted: 11 January 2016

References

- Chisholm S, Coaker G, Day B, Staskawicz B. Host-microbe interactions: shaping the evolution of the plant immune response. *Cell*. 2006;124(4):803–14.
- Dodds PN, Rathjen JP. Plant immunity: towards an integrated view of plant-pathogen interactions. *Nat Rev Genet*. 2010;11(8):539–48.
- Jones JDG, Dangl JL. The plant immune system. *Nature*. 2006;444(7117):323–9.
- Dangl JL, Horvath DM, Staskawicz BJ. Pivoting the plant immune system from dissection to deployment. *Science*. 2013;341(6147):746–51.
- Monaghan J, Zipfel C. Plant pattern recognition receptor complexes at the plasma membrane. *Curr Opin Plant Biol*. 2012;15(4):349–57.
- Bigeard J, Colcombet J, Hirt H. Signaling mechanisms in pattern-triggered immunity (PTI). *Mol Plant*. 2015;8(4):521–39.
- Stavrinos J, McCann HC, Guttman DS. Host-pathogen interplay and the evolution of bacterial effectors. *Cell Microbiol*. 2008;10(2):285–92.

8. Win J, Morgan W, Bos J, Krasileva KV, Cano LM, Chaparro-Garcia A, et al. Adaptive evolution has targeted the C-terminal domain of the RXLR effectors of plant pathogenic oomycetes. *Plant Cell*. 2007;19(8):2349–69.
9. Dong S, Stam R, Cano LM, Song J, Sklenar J, Yoshida K, et al. Effector specialization in a lineage of the Irish potato famine pathogen. *Science*. 2014;343(6170):552–5.
10. Ravensdale M, Nemri A, Thrall PH, Ellis JG, Dodds PN. Co-evolutionary interactions between host resistance and pathogen effector genes in flax rust disease. *Mol Plant Pathol*. 2011;12(1):93–102.
11. Allen RL. Host-parasite coevolutionary conflict between Arabidopsis and downy mildew. *Science*. 2004;306(5703):1957–60.
12. Kaschani F, Shabab M, Bozkurt T, Shindo T, Schornack S, Gu C, et al. An effector-targeted protease contributes to defense against *Phytophthora infestans* and is under diversifying selection in natural hosts. *Plant Physiol*. 2010;154(4):1794–804.
13. Meyers BC. Genome-wide analysis of NBS-LRR-encoding genes in Arabidopsis. *Plant Cell*. 2003;15(4):809–34.
14. Joshi RK, Nayak S. Perspectives of genomic diversification and molecular recombination towards R-gene evolution in plants. *Physiol Mol Biol Plants*. 2013;19(1):1–9.
15. Jacob F, Vernaldi S, Maekawa T. Evolution and conservation of plant NLR functions. *Frontiers Immunol*. 2013;4:297.
16. Sanseverino W, Ercolano MR. In silico approach to predict candidate R proteins and to define their domain architecture. *BMC Res Notes*. 2012;5:678.
17. Dangl JL, Jones JD. Plant pathogens and integrated defence responses to infection. *Nature*. 2001;411(6839):826–33.
18. Meyers B, Morgante M, Michelmore R. TIR-X and TIR-NBS proteins: two new families related to disease resistance TIR-NBS-LRR proteins. *Plant J*. 2002;32(1):77–92.
19. Staal J, Kaliff M, Dewaele E, Persson M, Dixelius C. RLM3, a TIR domain encoding gene involved in broad-range immunity of Arabidopsis to necrotrophic fungal pathogens. *Plant J*. 2008;55(2):188–200.
20. Nandety RS, Caplan JL, Cavanaugh K, Perroud B, Wroblewski T, Michelmore RW, et al. The role of TIR-NBS and TIR-X proteins in plant basal defense responses. *Plant Physiol*. 2013;162(3):1459–72.
21. Sarris PF, Duxbury Z, Huh SU, Ma Y, Segonzac C, Sklenar J, et al. A plant immune receptor detects pathogen effectors that target WRKY transcription factors. *Cell*. 2015;161(5):1089–100.
22. Le Roux C, Huet G, Jauneau A, Camborde L, Tremousaygue D, Kraut A, et al. A receptor pair with an integrated decoy converts pathogen disabling of transcription factors to immunity. *Cell*. 2015;161(5):1074–88.
23. Zhai C, Zhang Y, Yao N, Lin F, Liu Z, Dong Z, et al. Function and interaction of the coupled genes responsible for Pik-h encoded rice blast resistance. *PLoS One*. 2014;9(6):e98067.
24. Kanzaki H, Yoshida K, Saitoh H, Fujisaki K, Hirabuchi A, Alaux L, et al. Arms race co-evolution of Magnaporthe oryzae AVR-Pik and rice Pik genes driven by their physical interactions. *Plant J*. 2012;72(6):894–907.
25. Maqbool A, Saitoh H, Franceschetti M, Stevenson C, Uemura A, Kanzaki H, et al. Structural basis of pathogen recognition by an integrated HMA domain in a plant NLR immune receptor. *eLife*. 2015;25:4.
26. Jia Y, McAdams SA, Bryan GT, Hershey HP, Valent B. Direct interaction of resistance gene and avirulence gene products confers rice blast resistance. *EMBO J*. 2000;19(15):4004–14.
27. Cesari S, Thilliez G, Ribot C, Chalvon V, Michel C, Jauneau A, et al. The rice resistance protein pair RGA4/RGA5 recognizes the Magnaporthe oryzae effectors AVR-Pia and AVR1-CO39 by direct binding. *Plant Cell*. 2013;25(4):1463–81.
28. Ueda H, Yamaguchi Y, Sano H. Direct interaction between the tobacco mosaic virus helicase domain and the ATP-bound resistance protein, N factor during the hypersensitive response in tobacco plants. *Plant Mol Biol*. 2006;61(1–2):31–45.
29. Dodds PN, Lawrence GJ, Catanzariti A-M, Teh T, Wang C-IA, Ayliffe MA, et al. Direct protein interaction underlies gene-for-gene specificity and coevolution of the flax resistance genes and flax rust avirulence genes. *Proc Natl Acad Sci U S A*. 2006;103(23):8888–93.
30. Catanzariti A-M, Dodds PN, Ve T, Kobe B, Ellis JG, Staskawicz BJ. The AvrM effector from flax rust has a structured C-terminal domain and interacts directly with the M resistance protein. *Mol Plant Microbe Interact*. 2010;23(1):49–57.
31. Krasileva KV, Dahlbeck D, Staskawicz BJ. Activation of an Arabidopsis resistance protein is specified by the in planta association of its leucine-rich repeat domain with the cognate oomycete effector. *Plant Cell*. 2010;22(7):2444–58.
32. Chen Y, Liu Z, Halterman DA. Molecular determinants of resistance activation and suppression by *Phytophthora infestans* effector IPI-O. *PLoS Pathog*. 2012;8(3):e1002595.
33. Axtell MJ, Staskawicz BJ. Initiation of RPS2-specified disease resistance in Arabidopsis is coupled to the AvrRpt2-directed elimination of RIN4. *Cell*. 2003;112(3):369–77.
34. Mackey D, Holt 3rd BF, Wiig A, Dangl JL. RIN4 interacts with *Pseudomonas syringae* type III effector molecules and is required for RPM1-mediated resistance in Arabidopsis. *Cell*. 2002;108(6):743–54.
35. Ade J, DeYoung BJ, Golstein C, Innes RW. Indirect activation of a plant nucleotide binding site-leucine-rich repeat protein by a bacterial protease. *Proc Natl Acad Sci U S A*. 2007;104(7):2531–6.
36. Fujisaki K, Abe Y, Ito A, Saitoh H, Yoshida K, Kanzaki H, et al. Rice Exo70 interacts with a fungal effector, AVR-Pii, and is required for AVR-Pii-triggered immunity. *Plant J*. 2015;83(5):875–87.
37. van der Hooft RA, Kamoun S. From Guard to Decoy: a new model for perception of plant pathogen effectors. *Plant Cell*. 2008;20(8):2009–17.
38. Axtell MJ, Chisholm ST, Dahlbeck D, Staskawicz BJ. Genetic and molecular evidence that the *Pseudomonas syringae* type III effector protein AvrRpt2 is a cysteine protease. *Mol Microbiol*. 2003;49(6):1537–46.
39. Andersson MX, Kourtchenko O, Dangl JL, Mackey D, Ellerström M. Phospholipase-dependent signalling during the AvrRpm1- and AvrRpt2-induced disease resistance responses in Arabidopsis thaliana. *Plant J*. 2006;47(6):947–59.
40. Shao F, Golstein C, Ade J, Stoutemyer M, Dixon JE, Innes RW. Cleavage of Arabidopsis PBS1 by a bacterial type III effector. *Science*. 2003;301(5637):1230–3.
41. Mucyn TS, Clemente A, Andriotis VME, Balmuth AL, Oldroyd GED, Staskawicz BJ, et al. The tomato NBARC-LRR protein Prf interacts with Pto kinase in vivo to regulate specific plant immunity. *Plant Cell*. 2006;18(10):2792–806.
42. Ntoukakis V, Balmuth AL, Mucyn TS, Gutierrez JR, Jones AM, Rathjen JP. The tomato Prf complex is a molecular trap for bacterial effectors based on Pto transphosphorylation. *PLoS Pathog*. 2013;9(1):e1003123.
43. Cesari S, Bernoux M, Moncuquet P, Kroj T, Dodds PN. A novel conserved mechanism for plant NLR protein pairs: the “integrated decoy” hypothesis. *Frontiers Plant Sci*. 2014;5:606.
44. Wu CH, Krasileva KV, Banfield MJ, Terauchi R, Kamoun S. The “sensor domains” of plant NLR proteins: more than decoys? *Frontiers Plant Sci*. 2015;6:134.
45. Fukuoka S, Saka N, Koga H, Ono K, Shimizu T, Ebana K, et al. Loss of function of a proline-containing protein confers durable disease resistance in rice. *Science*. 2009;325(5943):998–1001.
46. Jupe F, Witek K, Verweij W, Sliwka J, Pritchard L, Etherington GJ, et al. Resistance gene enrichment sequencing (RenSeq) enables reannotation of the NB-LRR gene family from sequenced plant genomes and rapid mapping of resistance loci in segregating populations. *Plant J*. 2013;76(3):530–44.
47. Wessling R, Eppe P, Altmann S, He Y, Yang L, Henz SR, et al. Convergent targeting of a common host protein-network by pathogen effectors from three kingdoms of life. *Cell Host Microbe*. 2014;16(3):364–75.
48. Mukhtar MS, Carvunis AR, Dreze M, Eppe P, Steinbrenner J, Moore J, et al. Independently evolved virulence effectors converge onto hubs in a plant immune system network. *Science*. 2011;333(6042):596–601.
49. Steuernagel B, Jupe F, Witek K, Jones JD, Wulff BB. NLR-parser: rapid annotation of plant NLR complements. *Bioinformatics*. 2015;31(10):1665–7.
50. Jiao Y, Wickert NJ, Ayyampalayam S, Chanderbali AS, Landherr L, Ralph PE, et al. Ancestral polyploidy in seed plants and angiosperms. *Nature*. 2011;473(7345):97–100.
51. Adams KL, Wendel JF. Polyploidy and genome evolution in plants. *Curr Opin Plant Biol*. 2005;8(2):135–41.
52. Young ND, Debelle F, Oldroyd GE, Geurts R, Cannon SB, Udvardi MK, et al. The Medicago genome provides insight into the evolution of rhizobial symbioses. *Nature*. 2011;480(7378):520–4.
53. International Wheat Genome Sequencing Consortium (IWGSC). A chromosome-based draft sequence of the hexaploid bread wheat (*Triticum aestivum*) genome. *Science*. 2014;345(6194):1251788.
54. Velasco R, Zharkikh A, Affourtit J, Dhingra A, Cestaro A, Kalyanaraman A, et al. The genome of the domesticated apple (*Malus x domestica* Borkh.). *Nat Genet*. 2010;42(10):833–9.
55. Newman RM, Salunkhe P, Godzik A, Reed JC. Identification and characterization of a novel bacterial virulence factor that shares homology with mammalian Toll/interleukin-1 receptor family proteins. *Infect Immun*. 2006;74(1):594–601.

56. Ciril C, Wieser A, Yadav M, Duerr S, Schubert S, Fischer H, et al. Subversion of Toll-like receptor signaling by a unique family of bacterial Toll/interleukin-1 receptor domain-containing proteins. *Nat Med.* 2008;14(4):399–406.
57. Freeling M, Lyons E, Pedersen B, Alam M, Ming R, Lisch D. Many or most genes in *Arabidopsis* transposed after the origin of the order Brassicales. *Genome Res.* 2008;18(12):1924–37.
58. Kellogg EA. Evolutionary history of the grasses. *Plant Physiol.* 2001;125(3):1198–205.
59. Dardick C, Schwesinger B, Ronald P. Non-arginine-aspartate (non-RD) kinases are associated with innate immune receptors that recognize conserved microbial signatures. *Curr Opin Plant Biol.* 2012;15(4):358–66.
60. Dong J, Chen C, Chen Z. Expression profiles of the *Arabidopsis* WRKY gene superfamily during plant defense response. *Plant Mol Biol.* 2003;51(1):21–37.
61. Chi Y, Yang Y, Zhou Y, Zhou J, Fan B, Yu JQ, et al. Protein-protein interactions in the regulation of WRKY transcription factors. *Mol Plant.* 2013;6(2):287–300.
62. Rinerson CI, Rabara RC, Tripathi P, Shen QJ, Rushton PJ. The evolution of WRKY transcription factors. *BMC Plant Biol.* 2015;15:66.
63. Yamasaki K, Kigawa T, Watanabe S, Inoue M, Yamasaki T, Seki M, et al. Structural basis for sequence-specific DNA recognition by an *Arabidopsis* WRKY transcription factor. *J Biol Chem.* 2012;287(10):7683–91.
64. Kalde M, Barth M, Somssich IE, Lippok B. Members of the *Arabidopsis* WRKY group III transcription factors are part of different plant defense signaling pathways. *Mol Plant Microbe Interact.* 2003;16(4):295–305.
65. Hu Y, Dong Q, Yu D. *Arabidopsis* WRKY46 coordinates with WRKY70 and WRKY53 in basal resistance against pathogen *Pseudomonas syringae*. *Plant Sci.* 2012;185–186:288–97.
66. Wang D, Amornsiripanitch N, Dong X. A genomic approach to identify regulatory nodes in the transcriptional network of systemic acquired resistance in plants. *PLoS Pathog.* 2006;2(11):e123.
67. Goodstein DM, Shu S, Howson R, Neupane R, Hayes RD, Fazo J, et al. Phytozome: a comparative platform for green plant genomics. *Nucleic Acids Res.* 2012;40(Database issue):D1178–86.
68. Finn RD, Bateman A, Clements J, Coggill P, Eberhardt RY, Eddy SR, et al. Pfam: the protein families database. *Nucleic Acids Res.* 2014;42(Database issue):D222–30.
69. Eddy SR. Accelerated profile HMM searches. *PLoS Comput Biol.* 2011;7(10):e1002195.
70. Kim D, Pertea G, Trapnell C, Pimentel H, Kelley R, Salzberg SL. TopHat2: accurate alignment of transcriptomes in the presence of insertions, deletions and gene fusions. *Genome Biol.* 2013;14(4):R36.
71. Thorvaldsdottir H, Robinson JT, Mesirov JP. Integrative Genomics Viewer (IGV): high-performance genomics data visualization and exploration. *Brief Bioinform.* 2013;14(2):178–92.
72. Milne I, Stephen G, Bayer M, Cock PJ, Pritchard L, Cardle L, et al. Using Tablet for visual exploration of second-generation sequencing data. *Brief Bioinform.* 2013;14(2):193–202.
73. Edgar R. MUSCLE: multiple sequence alignment with high accuracy and high throughput. *Nucleic Acids Res.* 2004;32(5):1792–7.
74. Tamura K, Peterson D, Peterson N, Stecher G, Nei M, Kumar S. MEGA5: molecular evolutionary genetics analysis using maximum likelihood, evolutionary distance, and maximum parsimony methods. *Mol Biol Evol.* 2011;28(10):2731–9.
75. Zuckerkandl E, Pauling L. Molecules as documents of evolutionary history. *J Theor Biol.* 1965;8(2):357–66.
76. Felsenstein J. Confidence limits on phylogenies with a molecular clock. *Syst Zool.* 1985;34(2):152–61.
77. Pettersen EF, Goddard TD, Huang CC, Couch GS, Greenblatt DM, Meng EC, et al. UCSF Chimera—a visualization system for exploratory research and analysis. *J Comput Chem.* 2004;25(13):1605–12.

Submit your next manuscript to BioMed Central and we will help you at every step:

- We accept pre-submission inquiries
- Our selector tool helps you to find the most relevant journal
- We provide round the clock customer support
- Convenient online submission
- Thorough peer review
- Inclusion in PubMed and all major indexing services
- Maximum visibility for your research

Submit your manuscript at
www.biomedcentral.com/submit

